A climatological divide between wetness dominant and warmth dominant regimes of the vegetation in Siberia

*** Rikie SUZUKI, Jianqing XU, and Ken MOTOYA**
(Frontier Research Center for Global Change, Japan Agency for Marine-Earth Science and Technology)
***Frontier Research Center for Global Change,**
3173-25 Showamachi, Kanazawa, Yokohama, Kanagawa 236-0001, Japan
e-mail: rikie@jamstec.go.jp

Abstract

Wetness and warmth are the principal factors that control global vegetation distribution. This paper examines the normalized difference vegetation index (NDVI), warmth index (WAI), and wetness index (WEI) at a global scale, and investigates climate-vegetation relationships especially over Siberia. The NDVI was derived from a global, twenty-year AVHRR NDVI dataset with four-minute resolution. The WEI is defined as a fraction of precipitation to potential evaporation. The WAI is defined as the cumulative monthly mean temperature that exceeds 5°C annually. Meteorological data from the International Satellite Land-Surface Climatology Project, Initiative II (ISLSCP II) dataset were used to calculate WEI and WAI. All analyses used annual values based on averages from 1986 to 1995 at 1×1 degree resolution over land. Relationships between NDVI, WEI, and WAI values were examined using a vegetation-climate diagram with an orthogonal coordinate system using the WEI and the WAI. There are two major regimes in the vegetation-climate diagram for the NDVI, wetness dominant and warmth dominant. The boundary between the two regimes roughly corresponds to the vegetation boundary between taiga forest and southern vegetation over Siberia. The boundary occurs in areas where the NDVI is large and the maximum monthly temperature is around 18°C over Siberia.

Keyword: NDVI, NOAA/AVHRR, ISLSCP, Potential evaporation, Warmth index, Aridity

1. Introduction

The vegetation geographical distribution in terrestrial area in the world is strongly controlled by the climate (*e.g.*, Bonan, 2002). Especially, the wetness and warmth are the most essential factors that define the limitation of the vegetation distribution. We considers that almost all the vegetation in the world is stressed more or less by the dryness or low-temperature and it is possible to divide the world vegetation into wetness dominant and warmth dominant.

This study uses remotely-sensed Normalized Difference Vegetation Index (NDVI) data of the NOAA/AVHRR, and makes an attempt to divide the vegetation into two regimes, wetness dominant and warmth dominant, and demonstrates their distribution. The Wetness Index (WEI) and the Warmth Index (WAI) are calculated and their relation to the vegetation index is examined using a vegetation-climate diagram. Although the present study considers these relationships on global scales, the detail characteristics over Siberia will be discussed. Study results contribute to fundamental knowledge on regional vegetation and climate distributions and produce a baseline that can be used to predict vegetation change linked to future climate change.

2. Data and Method

All analyses occurred on a 1 × 1 degree grid over land using annual values based on a ten-year average from 1986 to 1995. The study area covers all land between 60°S and 80°N (that is, all land except for Antarctica and the Arctic).

2.1. Normalized Difference Vegetation Index

This study used 10-day NDVI data acquired from the global, 20-year, 4-minute-resolution AVHRR NDVI dataset (CEReS, 2001) produced by Chiba University. Monthly values were created from the 10-day NDVI values in the CEReS dataset by choosing the maximum NDVI in each month. The original 8-km grid cells were resampled to a 1 × 1-degree grid cell. NDVI values in winter are often meaningless because of low solar angle and snow cover. Therefore, annual values in this study were computed from monthly averaged NDVI values during the seven warmest months: March through September in the Northern Hemisphere, and September through March in the Southern Hemisphere.

2.2. Wetness Index (WEI)

The wetness index (WEI) is defined as the ratio of total precipitation to total potential evaporation during the warmest seven months. Potential evaporation, *Ep*, is defined in the present study as the evaporation expected from a continuously saturated surface (Kondo and Xu, 1997; Xu and Haginoya, 2001) for which surface roughness is assumed to be 0.005 m, albedo *ref* = 0.06 (water surface), surface emissivity ε = 0.98, and evaporation efficiency β^* = 1.0. Ground heat flux is neglected. According to the definition,

$$R^{\downarrow} = \varepsilon\sigma T_{SE}{}^4 + H + lE ,$$
$$H = c_p\rho C_H U\,(T_{SE} - T_A) ,$$
$$lE = l\rho\beta^* C_H U\,(h\, q_{SAT}(T_{SE}) - q_A)$$

where,

$$R^{\downarrow} = (1 - ref)\, S^{\downarrow} + \varepsilon L^{\downarrow}.$$

Here, $R^{\downarrow}$ is the input radiation at the ground surface. σ is the Stefan-Boltzmann constant (5.670×10^{-8} $Wm^{-2}K^{-4}$), and T_{SE} is the calculated surface temperature that satisfies the heat balance equations. Sensible heat flux H and latent heat flux lE are computed for the same time; c_p is the specific heat of air, and ρ is the air density. T_A is the air temperature, l is the latent heat of vaporization, h is the relative humidity (%), $q_{SAT}(T_{SE})$ is the specific humidity at saturation of T_{SE}, and q_A is the specific humidity of air. The evaporation rate E under these conditions is defined as the potential evaporation Ep. C_HU is the exchange speed, $C_HU = \mathrm{Max}[a + b \times 0.7U, c \times (T_{SE} - T_A)^{1/3}]$, where $a = 0.0027$ ms^{-1}, $b = 0.0031$, and $c = 0.0036$ $ms^{-1}K^{-3}$. The ratio Pa/Epa is the wetness index (WEI), where Pa and Epa are the total P and Ep during the warmest seven months.

A climatological value of the WEI for each pixel was calculated by averaging the WEI for 10 years in each 1 × 1-degree grid cell. The International Satellite Land Surface Climatology Project (ISLSCP) II (Hall *et al.*, 2004) dataset was used to calculate Pa and Epa.

Precipitation values were proportional to the values obtained every 6 hours from the National Centers for Environmental Prediction (NCEP) reanalysis. These NCEP values were adjusted so that the monthly totals corresponded to the monthly precipitation derived from precipitation gauge observations at the Global Precipitation Climatology Centre (GPCC). Moreover, systematic precipitation measurement errors linked to wind-induced under-catchment at rain gauges were compensated for using a method similar to empirical WMO formulas (Goodison *et al.*, 1989; Sevruk, 1982).

2.3. Warmth index (WAI)

To assess the climatological parameter of warmth, this study used a cumulative monthly temperature similar to the warmth index (WAI) of Kira's (1948) study on climatic zones and vegetation. The WAI is an annual, cumulative temperature of monthly mean temperatures exceeding 5°C. The WAI represents an effective temperature for vegetation and has been used in past studies of vegetation and temperature distributions. The WAI in each 1 × 1 degree grid cell was calculated using temperatures from the ISLSCP II dataset.

3. Relationship between NDVI, WEI, and WAI

Figure 1 shows a vegetation-climate diagram that includes the NDVI, WEI, and WAI in each 1 × 1-degree grid cell at global scale. Contours of the NDVI were superimposed on the figure after smoothing the NDVI distribution.

Large NDVI values match the regions where the WEI and WAI have large values in the diagram. For example, almost all NDVI values exceeding 0.4 occur where the WEI exceeds 0.3, and where the WAI exceeds 20°C. If the WEI is small, then the NDVI also has low values, corresponding to sparse vegetation in arid areas. Similarly, if the WAI is small, then the NDVI also has low values, corresponding to sparse vegetation in low temperature areas.

Plotted NDVI points fall into two main domains on the diagram. The first domain extends from the upper left corner to the upper right part of the diagram, and the second domain stretches from the lower right to the upper right. Vertically-drawn contours of the NDVI in the domain from the upper left to the upper right imply that the NDVI changes mainly with the WEI. In contrast, horizontally-drawn contours of the NDVI in the domain from the lower right to the upper right suggest that the NDVI changes mainly with the WAI.

4. Discussion

4.1. Vegetation regimes where wetness and warmth dominate

This section examines the implications of the two domains aforementioned. Figure 2 shows a smoothed slope of the NDVI against the WEI (G_{IE}) and WAI (G_{IA}) by a vector (declining direction of NDVI slope) at each plotted point in Fig. 1 About 1/10 points in Fig. 1 are selected to construct Fig. 2 for a clear picture. Those vectors were determined by a plain fitting (least square method) using NDVI, WEI, and WAI values which are in a smoothing circle.

Vectors in the upper part of the domain have a WEI-directed slope and vectors in the lower-right part of the domain have a WAI-directed slope. Wetness principally influences the NDVI in the upper domain; warmth dominates the NDVI in the lower-right domain. Global vegetation can therefore be partitioned into wetness- dominant and warmth-dominant regimes from a

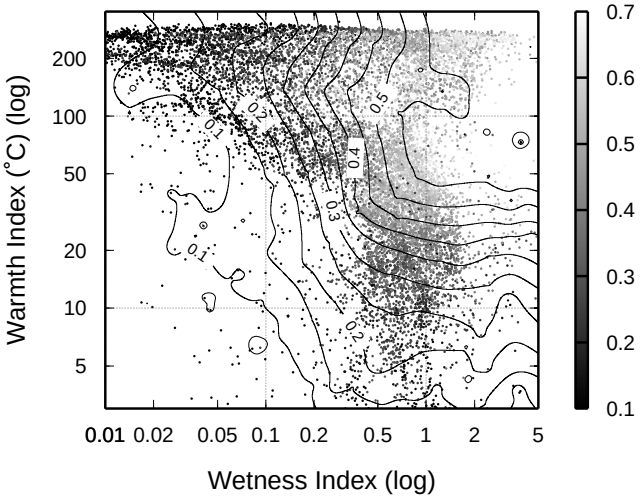

Fig. 1: The relationship between the NDVI, wetness index (WEI), and warmth index (WAI). The NDVI value (gray scale) at each 1 × 1-degree grid cell is plotted in the WEI-WAI orthogonal coordinate. The NDVI contours are drawn according to the smoothed NDVI distribution.

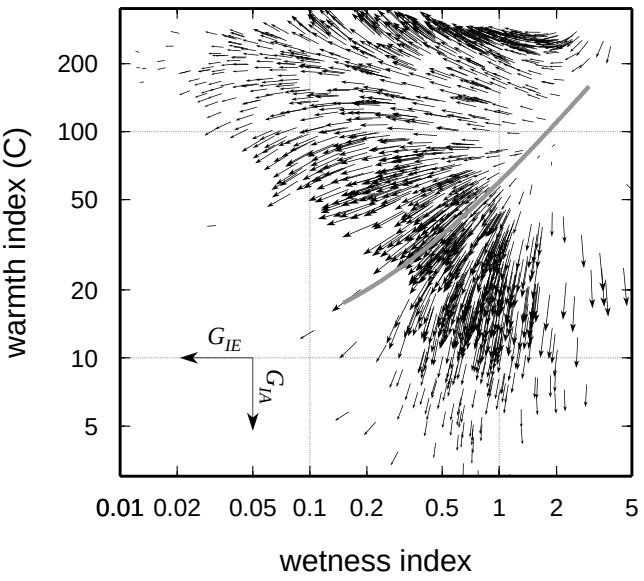

Fig. 2: Smoothed NDVI slope against the wetness index (WEI) and the warmth index (WAI). The gray line denotes the boundary between the wetness-dominant regime and the warmth-dominant regime.

macroscopic viewpoint. The grey line in Fig. 2 represents visually interpreted boundary between the two domains.

4.2. Geographical distribution of two regimes

Figure 3 shows the geographical distribution of the vectors which are the same in Fig. 2 but the direction was inverted for convenience sake. Most desert areas are absence from the vectors, because grid cells there have NDVI values of less than 0.1 and are therefore excluded from the slope calculation.

The two domains are clearly mapped in separate areas. At low- to mid-latitudes, most grid cells are dominated by wetness (horizontally-directed vectors), while at high latitudes in the Northern Hemisphere, warmth dominates (vertically-directed vectors). The boundary is along about 60°N line in Eurasia, corresponding to the boundary between boreal forest and cool forest/field.

4.3. Vegetation and climate in Siberia

Northern Asia clearly shows the boundary between wetness- and warmth-dominant regimes, as demonstrated in Fig. 3. Suzuki *et al.* (2000) discussed the meridional (south-north) distribution of vegetation in this area, considering two meridional transects from arid-to-taiga and taiga-to-tundra. NDVI values in the arid-to-taiga transect closely relate to the precipitation. NDVI values in the taiga-to-tundra transect closely relate to warmth. A subsequent paper, Suzuki *et al.* (2001), found maximum NDVI values over the zonal region where the maximum monthly temperature is around 18°C. The results of these previous studies suggest that the zone with maximum monthly temperatures around 18°C corresponds with the divide between wetness-dominant and warmth-dominant regimes.

Figure 4 shows the grid cells that have maximum monthly NDVI values (mean from 1986 to 1995) exceeding 0.7. Grid cells that have comparable NDVI slopes for the WEI and the WAI (the ratio of G_{IE} to G_{IA} is from 0.5 to 1.5) are superimposed on Fig. 4. Note that the zone of grid cells with maximum NDVI values over 0.7 agrees with the zone with comparable slopes of the WEI and the WAI. This demonstrates that the zone with high NDVI values, or the zone with temperatures around 18°C (Suzuki *et al.*, 2001), corresponds to the climatological divide between wetness-dominant and warmth-dominant vegetation regimes. Vegetation south of this zone is

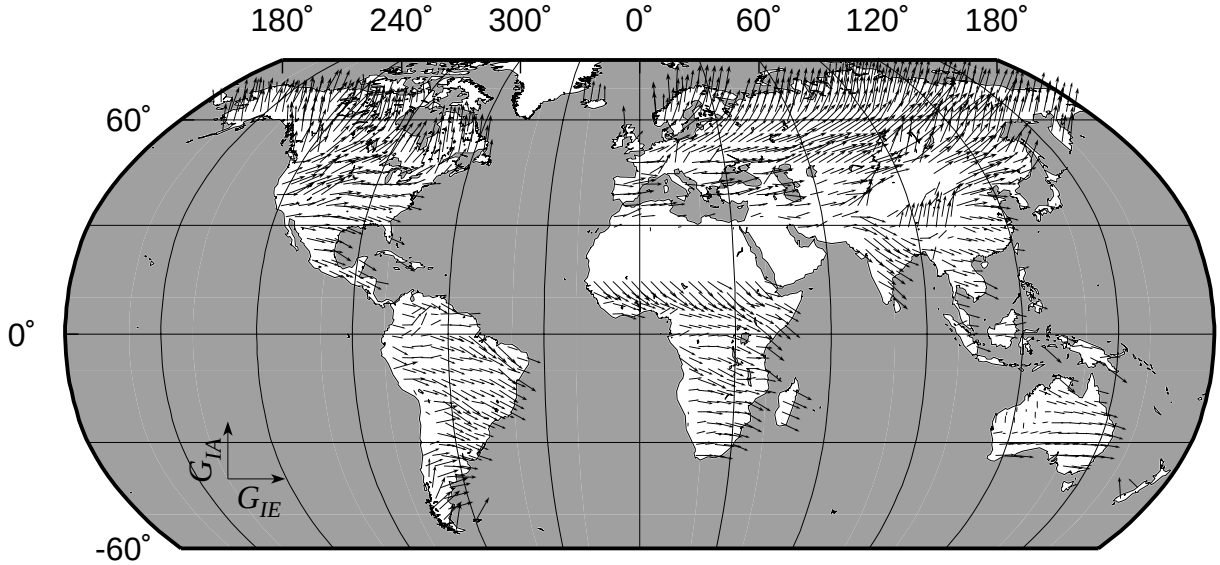

Fig. 3: The distribution of the slope of the NDVI against WEI (G_{IE}) and WAI (G_{IA}). The vector directions are inverted from those in Fig. 1. Vertical and horizontal directions of vectors correspond to the slope for WAI and WEI, respectively. Areas with NDVI values less than 0.1 are blank.

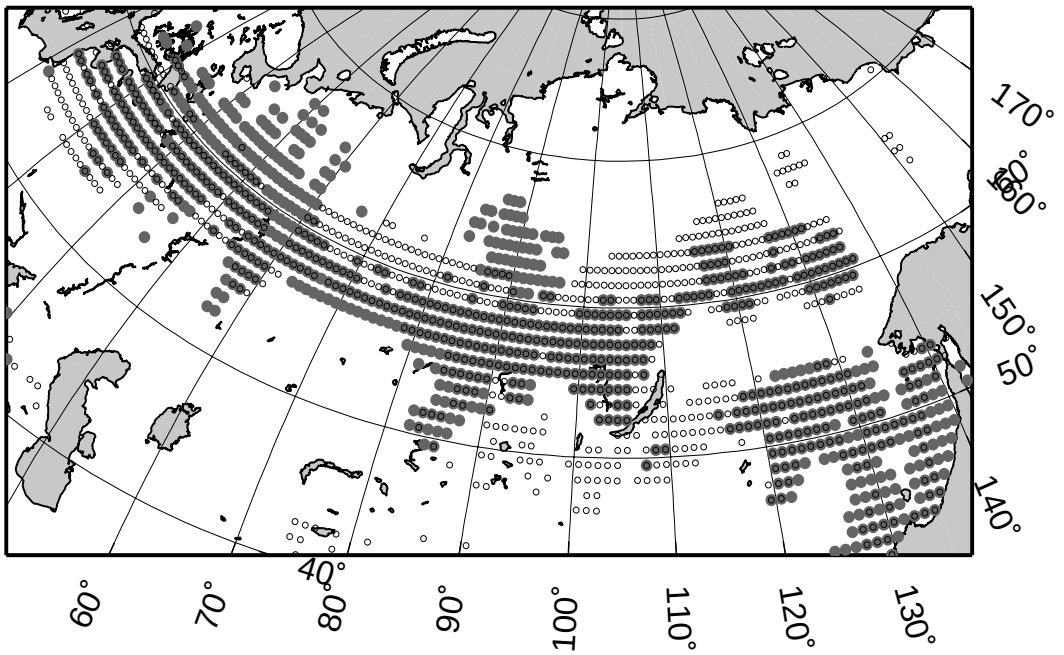

Fig. 4: The distribution of grid cells in which the maximum monthly NDVI exceeds 0.7 (gray circle), and the grid cells in which the NDVI slopes against the wetness index (WEI) and the warmth index (WAI) are comparable (the ratio of G_{IE} to G_{IA} is from 0.5 to 1.5) (small open circle).

constrained by aridity with higher temperatures than 18°C of maximum monthly temperature and small amounts of precipitation. Vegetation to the north of the zone is constrained by temperatures lower than 18°C.

5. Summary

Global NDVI distributions are related to two important climatological factors, wetness and warmth. The 10-year mean NDVI for the warmest seven months from 1986 to 1995 was calculated at 1 × 1-degree resolution using the CEReS NDVI dataset. The wetness index (WEI) and the warmth index (WAI) were defined and the 10-year mean WEI over the warmest seven months and the 10-year mean WAI were calculated using the ISLSCP II data. Geographic distributions of the NDVI, WEI, and WAI were transformed onto a vegetation-climate diagram, which uses the WEI and the WAI as orthogonal coordinates, to facilitate a discussion of the relationships among them.

There are two major vegetation regimes in the vegetation-climate diagram: wetness-dominant and warmth-dominant. The boundary between the two regimes roughly corresponds to the vegetation boundary between taiga forest and other southern vegetation. The boundary between the two regimes over northern Eurasia coincides with the high NDVI zone discussed by Suzuki *et al.* (2001). These results contribute to fundamental knowledge on regional vegetation and climate distributions and produce a baseline that can be used to predict vegetation change linked to future climate change.

References

Bonan G., *Ecological Climatology – Concepts and applications*. Cambridge University Press, Cambridge, 2002..

CEReS, Chiba University, *Twenty-year global 4-minute AVHRR NDVI Dataset*. Chiba University, Chiba, Japan, 2001.

Goodison, B.E., P.Y.T. Louie, and D. Yang, *WMO solid precipitation measurement intercomparison, final report*. WMO-872, 212pp, World Meteorological Organization, Geneva, 1989.

Hall, F.G., B. Meeson, S. Los, L. Steyaert, E. Brown de Colstoun, and D. Landis, eds. *ISLSCP Initiative II*. NASA. DVD/CD-ROM. NASA, 2004.

Kira, T., On the altitudinal arrangement of climatic zones in Japan —A contribution to the rational land utilization in cool highlands. *Agricultural Science of the North Temperate Region*, **2**, 143—173, 1948. (in Japanese)

Kondo, J, and J. Xu, Seasonal variations in the heat and water balances for non-vegetated surfaces. *J. Appl. Meteor.*, **36**,.1676—1695, 1997.

Sevruk, B., *Method of correction for systematic error in point precipitation measurement for operational use*. WMO-589, 91 pp, World Meteorological Organization, Geneva, 1982..

Suzuki, R., S. Tanaka, and T. Yasunari. Relationships between meridional profiles of satellite-derived vegetation index (NDVI) and climate over Siberia. *Int. J. Climatol.*, **20**, 955—967, 2000.

Suzuki, R., T. Nomaki, and T. Yasunari. Spatial distribution and its seasonality of satellite-derived vegetation index (NDVI) and climate in Siberia. *Int. J. Climatol.*, **21**, 1321—1335, 2001.

Xu, J., and S. Haginoya. An estimation of heat and water balances in the Tibetan Plateau. *J. Meteor. Soc. Japan*, **71**, 485—504, 2001.